Received: 18 November 2020 | Revised: 22 March 2021 | Accepted: 14 April 2021

DOI: 10.1111/mec.15931

ORIGINAL ARTICLE

MOLECULAR ECOLOGY WILEY

Environmental specialization and cryptic genetic divergence in two massive coral species from the Florida Keys Reef Tract

John P. Rippe[1] | Groves Dixon[1] | Zachary L. Fuller[2] | Yi Liao[1,3] | Mikhail Matz[1]

[1]Department of Integrative Biology, University of Texas at Austin, Austin, TX, USA

[2]Department of Biological Sciences, Columbia University, New York, NY, USA

[3]Department of Ecology and Evolutionary Biology, University of California Irvine, Irvine, CA, USA

Correspondence
John P. Rippe, Department of Integrative Biology, University of Texas at Austin, Austin, TX, USA.
Email: jpr6mg@gmail.com

Funding information
National Science Foundation, Grant/Award Number: OCE-1737312; Florida Keys National Marine Sanctuaries permit, Grant/Award Number: #2015-071

Abstract

Broadcast-spawning coral species have wide geographical ranges spanning strong environmental gradients, but it is unclear how much spatially varying selection these gradients actually impose. Strong divergent selection might present a considerable barrier for demographic exchange between disparate reef habitats. We investigated whether the cross-shelf gradient is associated with spatially varying selection in two common coral species, *Montastraea cavernosa* and *Siderastrea siderea*, in the Florida Keys. To this end, we generated a *de novo* genome assembly for *M. cavernosa* and used 2bRAD to genotype 20 juveniles and 20 adults of both species from each of the three reef zones to identify signatures of selection occurring within a single generation. Unexpectedly, each species was found to be composed of four genetically distinct lineages, with gene flow between them still ongoing but highly reduced in 13.0%–54.7% of the genome. Each species includes two sympatric lineages that are only found in the deep (20 m) habitat, while the other lineages are found almost exclusively on the shallower reefs (3–10 m). The two "shallow" lineages of *M. cavernosa* are also specialized for either nearshore or offshore: comparison between adult and juvenile cohorts indicates that cross-shelf migrants are more than twice as likely to die before reaching adulthood than local recruits. *S. siderea* and *M. cavernosa* are among the most ecologically successful species on the Florida Keys Reef Tract, and this work offers important insight into the genomic background of divergent selection and environmental specialization that may in part explain their resilience and broad environmental range.

KEYWORDS
adaptation, coral reef, ecological genomics, Florida Keys, speciation

1 | INTRODUCTION

Oceans continue to warm at a pace that many worry will threaten the sustainability of tropical coral reefs within the next 50–100 years (Hoegh-Guldberg et al., 2007). Major coral bleaching events are occurring with increasing frequency, compounding the loss of living coral cover year after year (Hughes et al., 2017). The severity of this decline is prompting reef managers to consider proactive measures designed to enhance coral adaptation to heat stress. Examples of such measures include assisted gene flow, or the injection of adaptive alleles into threatened populations via hybridization with corals from warmer environments, and selective breeding and outplanting of individuals that demonstrate elevated resilience to thermal stress (Hagedorn et al., 2018; Quigley et al., 2019; van Oppen et al., 2015, 2017).

To predict the success of these actions and understand the evolutionary potential of coral reefs more generally, the patterns by which genetic variation is naturally distributed and exchanged among individuals on the reef must be evaluated. Coral populations on modern reefs have endured the selective pressure of decades of environmental change and therefore offer valuable insight into the factors driving the segregation and sorting of genetic diversity.

Yet, while conventional surveys of broad-scale population genetics provide a useful introduction to the genetic landscape of a study species, often the most pertinent follow-up questions are left unresolved. What are the genetic processes underlying local adaptation and population differentiation in scleractinian (i.e., stony) corals? What mechanisms may be restricting the exchange of genetic material between divergent populations? To ensure lasting success in restoration activities and the efficient use of limited resources, it will be imperative to take these factors into account.

Complicating this task immensely is the incomplete and often muddled picture of speciation and diversification in corals. Rapid advances in DNA sequencing have ushered in a wave of genomic data sets, which have revealed that species boundaries originally defined based on morphological characteristics are often not consistent with inferences based on experimental and population genetic evidence (Willis et al., 1997). Interspecific hybridization, for example, is prevalent within many coral genera (reviewed by Willis et al., 2006). This has fueled debate on the relevance of reticulate evolution (Vollmer & Palumbi, 2002), the notion that speciation in scleractinian corals is a fluid process involving backcrossing and migration among diverged lineages. On the other hand, apparent lack of gene flow and reproductive isolation within certain species has led to suggestions that cryptic speciation may be more common in corals and related taxa than is currently recognized (Bongaerts et al., 2010a; Ladner & Palumbi, 2012; Richards et al., 2016; Rosser, 2015; Schmidt-Roach et al., 2013; Warner et al., 2015). Together, these dynamics can have important implications on the exchange of genetic variation, and of adaptive alleles more specifically, among coral populations.

One important process that can lead to genetic divergence is local adaptation due to spatially varying selection across an environmental gradient. It was long presumed that due to large dispersal distances and few apparent physical barriers to gene flow, most marine organisms were well mixed genetically across their range, with high migration rates largely swamping out the development of local adaptation (Ronce & Kirkpatrick, 2001). While there is evidence for such high gene flow in some marine systems, for many other species population connectivity is considerably lower than previously thought, suggesting that high gene flow is not a general trend (reviewed in Palumbi, 2004). In reef-building corals, local adaptation is often inferred from *ex situ* or reciprocal transplant experiments in which individuals tend to perform better in conditions most similar to their environment of origin (Barkley et al., 2017; Howells et al., 2013; Kenkel et al., 2013, 2015). Several recent studies have linked these patterns to a genetic basis (Dixon et al., 2015; Palumbi et al., 2014), but the specifics of this association are not well resolved. Thus, there is still much left unknown about the prevalence of local adaptation in stony corals and the underlying genetic mechanisms that maintain it.

Here we study two coral species, *Montastraea cavernosa* and *Siderastrea siderea*, which are ubiquitous in the wider Caribbean. We sampled two age cohorts (juveniles and adults) of each species across three sites representing a cross-shelf gradient in the lower Florida Keys: a shallow nearshore, shallow offshore and deep offshore reef environment. Each reef zone represents a unique set of limiting environmental conditions that have a demonstrated effect on coral fitness (Kenkel et al., 2013; Lirman & Fong, 2007). With this in mind, we expected to see evidence of spatially varying selection among reef zones, manifesting as an increase in genetic differentiation in the adult cohort compared to the juvenile cohort. In particular, considering that both coral species are broadcast-spawners with the dispersal potential vastly exceeding the spatial scope of our sampling, we expected to see this effect only at a minority of loci in the genome involved in local adaptation.

2 | MATERIALS AND METHODS

2.1 | Sample collection and site features

Samples were collected from two massive coral species, *Montastraea cavernosa* and *Siderastrea siderea*, from three sites along the cross-shelf gradient in the lower Florida Keys (Figure 1a). Each sampling site typifies a unique environmental setting: (i) a shallow nearshore patch reef (3–5 m) adjacent to Summerland Key on the shoreward boundary of Hawk Channel (24.607°N, 81.429°W), (ii) a shallow offshore site (~10 m) representing a backreef community adjacent to the relict barrier reef structure of the Florida Keys Reef Tract (24.553°N, 81.438°W), and (iii) a deep offshore site (~20 m) near the base of the reef slope seaward of the Looe Key Sanctuary Preservation Area (24.541°N, 81.414°W). These habitats differ substantially in their ambient environmental conditions, in that nearshore reefs experience on average greater terrestrial influence (i.e., higher turbidity, dissolved nutrient levels and chlorophyll *a* and larger temperature fluctuations than offshore reefs (Lirman & Fong, 2007). Exposure to the Florida Current maintains a relatively stable temperature regime in both offshore habitats, although greater depth is associated with lower levels of photosynthetically active radiation (Lesser, 2000).

At each sampling site, small tissue fragments were collected from 20 adults and 20 juveniles of each species when possible. In some cases, 20 individuals of both life stages could not be located, leaving a total sample size of 118 for *M. cavernosa* and 123 for *S. siderea*. Life stages were distinguished based on colony diameter, with colonies larger than 30 cm across classified as adults, and those smaller than 3 cm classified as juveniles. All samples were preserved in 100% ethanol at −20°C until transport to the University of Texas at Austin, where they were kept at −80°C until processing.

2.2 | Montastraea cavernosa genome assembly and annotation

One specimen of *M. cavernosa* was collected for genome sequencing from the West Bank of the Flower Garden Banks Marine Sanctuary (27.88°N, 93.83°W). We constructed a *de novo* genome assembly of *M. cavernosa* using a combination of PacBio reads and Illumina paired-end reads with 10X Genomics Chromium barcodes. The

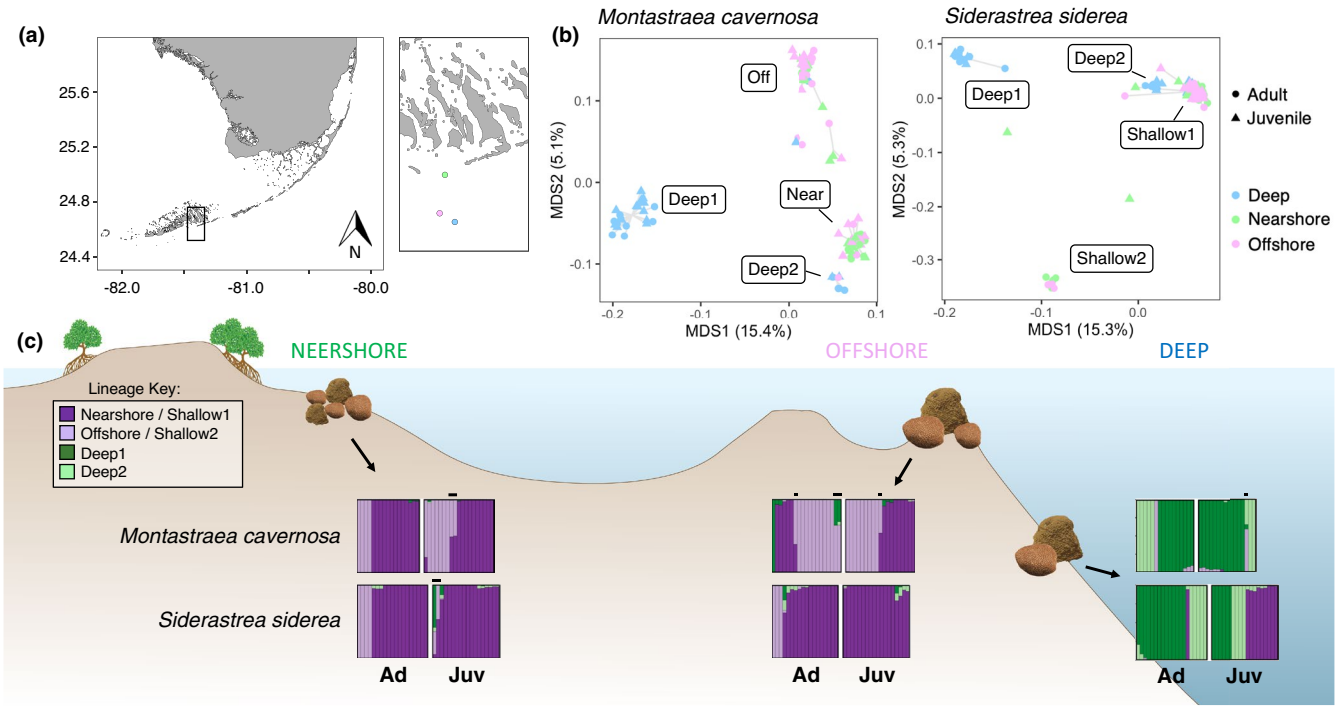

FIGURE 1 Sample map and spatial population genetics. (a) The three sampling sites (Nearshore: green, Offshore: pink, Deep: blue) are displayed in the inset map. (b) Principal coordinate analyses (PCoA) demonstrate the four distinct lineages evident within each species. The colors of individual points correspond to the habitats specified in the sample map. (c) Admixture plots for each species are displayed along the bathymetric cross-section diagram, separated by adults (A) and juveniles (J) in each habitat. Note the four distinct lineages in each species, two distributed primarily across the shallow nearshore and offshore sites and two restricted to the deep. Throughout the text, lineages are referenced as follows: Nearshore / Shallow1 (dark purple, *M. cavernosa* / *S. siderea*), Offshore / Shallow2 (light purple, *M. cavernosa* / *S. siderea*), Deep1 (dark green), Deep2 (light green). Hybrids with >25% ancestry to a secondary lineage are indicated with black bars above the plots

PacBio sequencing (nine SMRT cells, yielding 1.9 million subreads with N50 = 8kb, 15.7 Gb total) was performed at the Duke Center for Genomic and Computational Biology. 10X barcode libraries were generated and paired-end reads were sequenced on an Illumina HiSeqX platform at the New York Genome Center.

Our assembly approach follows a similar method used to generate a reference genome for the coral *Acropora millepora* (Fuller et al., 2020) and is described in detail along with the annotation pipeline in the Supporting Methods.

2.3 | Reduced representation library preparation and sequencing

Genomic DNA was extracted from tissue samples using a modified phenol–chloroform procedure, and samples were prepared for reduced-representation sequencing using the 2bRAD methodology (Wang et al., 2012). The latest version of the protocol, employing the triple-barcoding scheme and degenerate tags for identification of PCR (polymerase chain reaction) duplicates, is available at https://github.com/z0on/2bRAD_denovo. In addition, specific details of this protocol and of the DNA extraction method used in this study can be found in the Supporting Methods. All samples were pooled and sequenced on the Illumina HiSeq 2500 platform at the University of Texas at Austin DNA Sequencing Facility.

2.4 | Data filtering and genotyping

Raw sequencing reads were trimmed of adaptors and demultiplexed using a custom script (https://github.com/z0on/2bRAD_denovo/blob/master/trim2bRAD_2barcodes.pl) and were quality filtered using the program CUTADAPT version 1.14 (Martin, 2011), removing any reads with a Phred score of less than 15 at either end. Because *S. siderea* lacks a published genome assembly, a reference was generated *de novo* for genotyping. To do so, sample reads were first mapped to an aggregate genome comprising the four Symbiodiniaceae genera *Symbiodinium*, *Breviolum*, *Cladocopium* and *Durusdinium* (Aranda et al., 2016; Dougan, 2020; H. Liu et al., 2018; Shoguchi et al., 2013) using the program BOWTIE2 version 2.3.4 (Langmead & Salzberg, 2012). Any reads that mapped successfully with a minimum end-to-end alignment score of −22.2 were removed so that those left behind could be assumed to belong to the coral host. The program CD-HIT version 4.8.1 (Fu et al., 2012) was then used in combination with custom Perl scripts (https://github.com/z0on/2bRAD_denovo) to cluster and assemble reads from the 60 samples with the highest

remaining sequencing coverage into a reference genome with 30 equally sized pseudochromosomes for mapping.

Using this *de novo* assembly for *S. siderea* and the *M. cavernosa* genome described above (https://matzlab.weebly.com/data--code.html), sample reads were mapped to the appropriate reference using BOWTIE2 (Langmead & Salzberg, 2012). Samples with greater than 25% of reads successfully aligned and at least 5× sequencing depth for more than 25% of loci were retained for further analyses. Those failing to pass both filters were removed (*S. siderea*: $n = 5$, *M. cavernosa*: $n = 6$). Alignment files were sorted and converted to BAM format using SAMTOOLS version 1.6 (Li et al., 2009).

All genotyping and identification of single nucleotide polymorphisms (SNPs) was performed using the ANGSD program suite version 0.933-25 (Kim et al., 2011; Korneliussen et al., 2014; Nielsen et al., 2012), which is well suited for low-coverage genetic data as it operates on genotype likelihoods, rather than hard genotype calls, in most downstream applications.

Lastly, prior to any population genetic analyses, samples representing genetically identical individuals (i.e., generated via asexual reproduction) were identified based on the degree of genetic dissimilarity as compared to technical replicates included in the sample set (i.e., separate sequencing libraries prepared from the same tissue sample). To do so, variant sites (biallelic SNPs) were identified under a stringent filtering scheme in order to ensure confidence in polymorphic loci—all loci were required to have a base call quality greater than Q25, mapping quality greater than Q20, an SNP *p*-value less than 1×10^{-5}, a minimum minor allele frequency of 0.05 and be sequenced in at least 80% of samples. Based on these loci (*M. cavernosa*: 8,039 SNPs, *S. siderea*: 13,016 SNPs), pairwise identity-by-state (IBS) distance was calculated between all samples, and a hierarchical clustering tree was constructed using the function *hclust* in R version 3.6.1 (R Core Team, 2019) to distinguish genetically identical individuals. Any samples exhibiting a genetic dissimilarity as low as known technical replicates were assumed to be genetically identical, and only the individual of each clonal group with the greatest total read count was chosen to be retained for further analyses ($n = 2$ samples removed per species; Figure S1). All the scripts and detailed outline of the bioinformatic procedures are available at https://github.com/z0on/2bRAD_denovo.

2.5 | Population structure

Genome-wide population structure was assessed in each species using two methods: (i) individual admixture proportions among K inferred ancestral lineages, and (ii) principal component analysis based on IBS distance. First, variant sites were identified using the ANGSD filters described above—here, the requirement for a locus to be sequenced in 80% of samples reflects the reduced sample size after genetically identical individuals were removed (*M. cavernosa*: 8,265 SNPs, *S. siderea*: 14,827 SNPs). Based on variation at these loci and given a specified number of ancestral lineages ($K = 2–6$) in the population, the proportion of each individual's ancestry derived from each inferred lineage was estimated using the programs NGSADMIX version 3.2 (Skotte et al., 2013) and PCANGSD (Meisner & Albrechtsen, 2018). The results of these two analyses are virtually identical, identifying four clearly distinct lineages within each species. Only the NGSADMIX results are presented in Figure 1, but a comparison of the two analyses can be seen in Figure S2. Additionally, to compare and corroborate the interpretation of this analysis, pairwise IBS distance between individuals was calculated in ANGSD. Principal coordinate analysis (PCoA) was performed on the resulting matrix using the *vegan::capscale* function in R (Oksanen et al., 2019) to visualize the clustering of samples with respect to the major axes of genetic variation. The four distinct genetic lineages identified within each species based on the combination of these results form the basis for all subsequent analyses.

2.6 | Modelling demographic histories

To infer the demographic history of these genetic lineages, we used two approaches based on allele frequency spectra (AFS), both aiming to reconstruct demographic scenarios that most accurately reproduce the observed AFS. For both analyses, target loci were identified using modified filters in ANGSD in order to retain all well-sequenced sites, including invariant ones (Matz, 2018). Modifications include increasing the minimum sequencing and mapping quality to Q35 and Q30, respectively, while removing the minimum allele frequency and minimum SNP *p*-value filters. These additional filters returned roughly a million sites for each species and did not qualitatively change our conclusions of population structure (Figure S3). AFS were then generated using ANGSD for the four genetic lineages that were identified in each species, using only samples that had less than 25% of alternative lineage ancestry as determined by NGSADMIX (*M. cavernosa*: $n = 99$ [seven putative hybrids removed], *S. siderea*: $n = 110$ [two putative hybrids removed]).

Since the reference genome for *M. cavernosa* was sampled from an outlying population in terms of both geographical distance and habitat type (near-mesophotic deep habitat in the Flower Garden Banks in the Gulf of Mexico), we assumed the alleles not matching the reference to be derived in the populations studied here. To correct for possible misidentification of ancestral and derived allelic states, two-dimensional demographic models included the proportion of misidentified ancestral states as a free parameter. Since *S. siderea* lacks a reference genome, alleles cannot be polarized into ancestral and derived states; thus, all AFS were "folded" at a minor allele frequency of 0.5.

To reconstruct the history of effective population size changes for each genetic lineage, we applied STAIRWAYPLOT version 2 (X. Liu & Fu, 2015) to one-dimensional AFS. STAIRWAYPLOT is an unsupervised analysis that does not require prespecified demographic models. Prior to this analysis, we used BAYESCAN (Foll & Gaggiotti, 2008) to identify F_{ST} outliers (i.e., sites showing more allele frequency divergence between genetic lineages than expected under a neutral island model). BAYESCAN was run using default settings: 20 pilot runs

(5,000 iterations in length) followed by a burn-in of 50,000 iterations and a final run of 100,000 iterations. Sites that were assigned a q-value of <0.5 for being an F_{ST} outlier were removed, leading to removal of 6.4 % and 5.2% of all sites for *M. cavernosa* and *S. siderea*, respectively. Such a permissive q-value threshold was chosen to ensure that all potentially non-neutral sites were removed, following Matz et al. (2018).

Additionally, we used the *Moments* Python library (Jouganous et al., 2017; Gravel, n.d.) based on two-dimensional AFS to estimate not only population size changes, but also the timing and magnitude of introgression between each pair of genetic lineages. Unlike STAIRWAYPLOT, the *Moments* modelling workflow requires demographic models to be specified at the outset, which are defined and executed using custom Python scripts. Here, we specified a set of 108 different models that represent a wide range of possible demographic scenarios—notable differences between models include variations in the occurrence and timing of symmetric or asymmetric migration, the timing and dynamics of population size changes, and crucially, whether migration rates are allowed to vary across the genome to represent "islands of differentiation" (Duranton et al., 2018).

The *Moments* procedure followed three main steps to ensure confidence in model selection and parameter estimation. (i) First, 100 bootstrapped two-dimensional AFS were generated using ANGSD for each pairwise population comparison. For *M. cavernosa*, bootstrapping was done by resampling genomic scaffolds; for *S. siderea*, pseudochromosomes from the read-based reference. For 10 of these AFS, each of the 108 demographic models was run six times with randomly chosen initial parameter values to ensure that each model converges to its optimum on each replicate at least once. (ii) Following Burnham and Anderson (2002), model log likelihoods were then converted to Akaike's information criterion (AIC) using the formula:

$$AIC = -2(\log(L)) + 2K$$

where L is the likelihood of the model and K is the number of model parameters. The best-fit run of each model (out of six) on each bootstrap replicate was identified, and from this set, the demographic model with the lowest median AIC across the 10 bootstrap replicates was determined. (iii) Lastly, this model was fitted to all 100 bootstrapped AFS in order to estimate the confidence of demographic parameters. Again, six random restarts per bootstrap replicate were performed, each of them initiated by randomly perturbing the parameters estimated at the model selection stage. All *Moments* models, accessory scripts and instructions for this procedure are available at https://github.com/z0on/AFS-analysis-with-moments.

Estimated parameters (T, θ, M) were converted to time in years (t), effective population size in number of individuals (N_e), and migration rates as the fraction of the total population that are new immigrants per generation (m) assuming a mutation rate of 2×10^{-8} per base per generation and a generation time of 5 years (Matz et al., 2018). We note that the mutation rate has been measured for a different coral genus (*Acropora*) and is therefore just a rough approximation (Richards et al., 2013). This makes our estimates of absolute values of time and population sizes unreliable; however, relative differences, such as population size changes or differences in migration rates, are as accurate as the models' parameter estimates. Additionally, for both AFS-based analyses, AFS were down-projected to 80% of the actual number of genomes within each population to reduce the noise in the higher-frequency region typical for ANGSD-derived AFS.

2.7 | Identifying loci underlying population structure

To investigate the genomic organization and association of loci underlying population differentiation, we introduce a novel method that we call "LD networks," which is an application of weighted gene co-expression network analysis (WGCNA) to genotyping data based on the measurement of genotype correlation between pairs of SNPs. WGCNA was originally developed for analysis of gene expression (Langfelder & Horvath, 2008), to identify groups of genes that exhibit similar expression dynamics across samples (i.e., consistently up- or down-regulated together). The LD networks approach applies this methodology to identify groups of *loci* that demonstrate correlated changes in *genotype* across samples. In this case, rather than using the correlation of expression between genes, the adjacency matrix at the core of network construction consists of the pairwise linkage disequilibrium (LD) between loci. The characteristics of resulting "SNP modules" and associated changes in allele frequency are then evaluated with respect to sample-specific traits and metadata. In a way, this methodology is equivalent to local principal components analysis (PCA) (Li & Ralph, 2019) with single-base resolution: it identifies parts of the genome that show alternative versions of population structure, but instead of grouping genomic windows (as in the local PCA method) it groups individual SNP loci.

The analysis required five steps: (i) SNPs were first identified using the same ANGSD filters as were used to characterize population structure. Posterior genotype probabilities at each locus were estimated, recorded as the probability of each individual to carry zero, one or two derived alleles with respect to the reference genome (i.e., 0: homozygote ancestral, 1: heterozygote, 2: homozygote derived). For *S. siderea*, in the absence of a proper reference assembly, all minor alleles were assumed to be derived. This information is converted into a single value of derived alleles by multiplying each probability by its corresponding genotype and adding together. (ii) Genomic coordinate information was then used to filter SNPs assumed to be physically linked. For *M. cavernosa*, a linkage block was defined as any group of SNPs in which the distance between subsequent loci was less than 1,000 bp. Here, the goal is not to completely remove linked sites, but rather to disregard correlations caused by close proximity of loci, to focus on longer range correlations that might be caused by biologically interesting factors. For *S. siderea*, the relative genomic position of RAD tags is unknown, so linked sites could only be identified as those within 36 bp of each other (i.e., the size of a single RAD tag). For each linkage block, the SNP with the

highest minor allele frequency was retained and all others were removed from further analysis. (iii) Pairwise coefficient of variation (R^2) was calculated for all remaining SNPs with a minor allele frequency exceeding 0.05 using the Expectation-Maximization algorithm in NGSLD version 1.1.0 (Fox et al., 2019). The resulting matrix of correlation values is equivalent, in WGCNA terms, to an unsigned adjacency matrix based on a soft thresholding power of 2. This matrix was then used as input to the WGCNA function *TOMsimilarity*, to calculate the topological overlap matrix reflecting the sharing of the "correlation neighborhood" among loci. This and all further steps in this analysis were implemented using the WGCNA version 1.69 package in R (Langfelder & Horvath, 2008). (iv) Following network construction, distinct groups (or "modules") of SNPs with covarying genotypes across samples were identified using unsupervised hierarchical clustering in combination with the Dynamic Tree Cut method. (v) Lastly, association of the SNP modules with sample metadata were explored. This analysis was based on module "eigengenes," which represent the first principal component of the genotype matrix for all SNPs included in a module. Eigengene values across samples were regressed against the samples' metadata: assignment to a specific genetic lineage, sampling site and age cohort. Additional analysis on module–metadata association was based on the fact that not all SNPs included in the module are equal: each SNP is assigned the "module membership," called "kME" in WGCNA terms, which is the correlation between the SNP genotype and the eigengene of the module. Greater kME indicates that an SNP is highly representative of the module's behaviour across samples and is likely to be among the primary responders to the factor(s) driving the correlation between SNPs within the module.

A chi-squared test was used to determine if SNPs of each module showed evidence of clustering throughout the genome. The proportion of total SNPs expected to occur within each scaffold of the genome assembly was calculated by simply dividing the number of SNPs within each scaffold by the total number of SNPs in the data set. For each module, the expected number of SNPs within each scaffold was then calculated as the product of the expected proportion above and the total number of module SNPs. A comparison of the observed and expected number of module SNPs within each scaffold was used as the basis for the chi-squared significance test. Because *S. siderea* lacks a proper genome assembly, this analysis was only performed for *M. cavernosa*.

Additionally, to explore the possible functional significance of each module, we identified SNPs that fell within 2,000 bp of annotated gene boundaries and conducted a rank-based gene ontology (GO) enrichment analysis using the GO_MWU method (Wright et al., 2015; https://github.com/z0on/GO_MWU). GO_MWU is particularly powerful for WGCNA modules because it performs a two-layered test: first, a Fisher's exact test for presence–absence of GO-annotated genes in the module, and second, a within-module Mann–Whitney U-test to determine whether the GO-annotated genes rank consistently near the top of the list of module membership values. Overall significance is assessed based on random permutations. Again, this analysis was only performed for *M. cavernosa*.

2.8 | Locus-specific F_{ST}

Based on the outcome of the WGCNA analysis, we hypothesized that SNPs exhibiting highest membership to each module are in fact those that are most strongly differentiated between lineages. To evaluate this hypothesis, we estimated locus-specific F_{ST} in two ways. First, the *realSFS* function in ANGSD was used to calculate locus-specific F_{ST} for each pairwise comparison of the four genetic lineages in each species. F_{ST} values from all pairwise comparisons including each lineage were averaged to produce four lineage-specific F_{ST} estimates for every SNP. Second, a Bayesian F_{ST} outlier test was implemented in BAYESCAN version 2 (Foll & Gaggiotti, 2008). Outlier loci were identified as those in which the false discovery rate-corrected q-value based on the posterior probability of the selection model was less than 0.05. Linear correlation was used to compare SNP module membership to F_{ST} estimates, with the expectation that loci exhibiting the highest membership to each module will also exhibit the highest F_{ST} values for the module-associated lineage and will be identified by BAYESCAN as F_{ST} outliers.

3 | RESULTS

3.1 | Population structure

Montastraea cavernosa and *Siderastrea siderea* exhibit remarkably similar patterns of population structure across the three reef zones. Admixture analysis and IBS-based genetic distance indicate that both species comprise four distinct lineages. Two lineages occur almost exclusively in the deep habitat and two are primarily distributed across the shallow nearshore and outer reef habitats (Figure 1b,c; Figure S4). Admixed individuals with more than one source of ancestry are rare—only seven and two individuals of *M. cavernosa* and *S. siderea*, respectively, exhibit more than 25% ancestry from a secondary lineage (Figure 1b,c). Global F_{ST} between lineages ranges from 0.06 to 0.19 in *M. cavernosa* and 0.07 to 0.25 in *S. siderea* (Figure 2a; Table S1). There is no consistent spatial pattern in the magnitude of differentiation—in *M. cavernosa*, the two sympatric deep populations exhibit the highest F_{ST} of all comparisons, and in *S. siderea*, the lowest F_{ST} is observed between one of the deep and one of the shallow lineages (Figure 2a; Table S1).

Comparing the genetic structure of adult and juvenile cohorts within each habitat reveals a degree of local adaptation. In *M. cavernosa*, juveniles of light and dark purple ancestry occur at relatively equal abundance at the nearshore and offshore sites (7:10 and 9:9, respectively; Figure 1c), while adult populations in each environment shift predominantly to one or the other.

Specifically, adults of dark purple ancestry outnumber those of light purple ancestry 13:4 in the nearshore environment, but are outnumbered 5:12 in the offshore environment (Figure 1c). Assuming a constant recruitment rate across the two generations, we can calculate the relative fitness of each ancestral lineage in the two environments as:

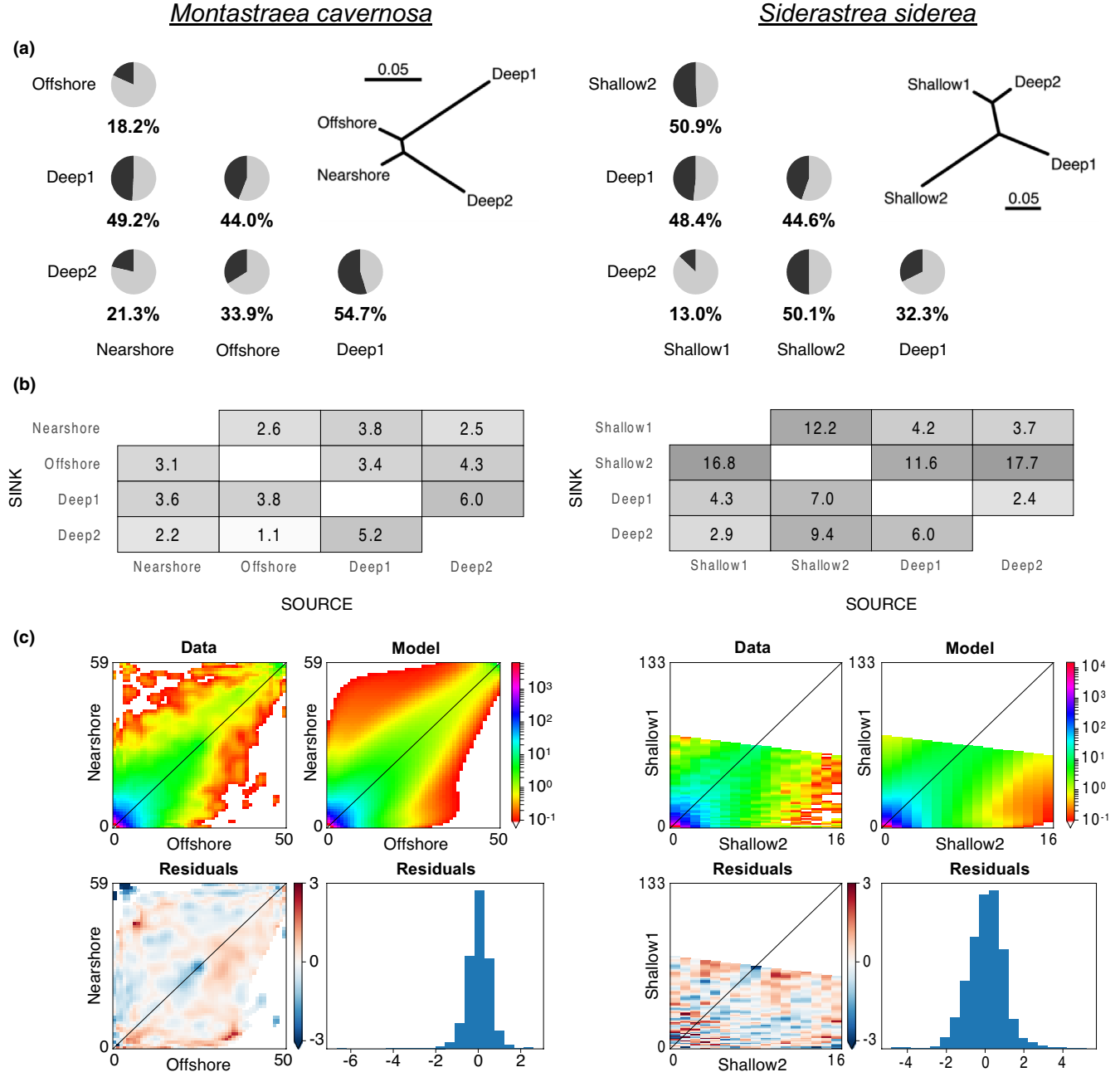

FIGURE 2 Demographic modelling indicates reduced gene flow in a substantial proportion of the genome. (a) Pie charts depict the proportion of the genome experiencing lower introgression rate between each population pair compared to the rest of the genome ("islands of differentiation"). Distance trees reflecting the global mean pairwise F_{ST} between lineages are displayed in the top right corner of this panel. (b) Fold change by which the introgression is reduced at the islands of differentiation. Box shading reflects the magnitude of reduction. (c) Diagnostic plots showing the goodness-of-fit of one of the six pairwise demographic models for each species. The top two panels show the observed allele frequency spectra (AFS) (left) and the modelled AFS (right); the lower two panels show model errors plotted as residuals in the AFS space (left) and as a histogram (right). All demographic models include a parameter allowing variation in the migration rate across the genome

$$\frac{P_{A\,(t=1)}}{P_{A\,(t=0)}} \Big/ \frac{P_{B\,(t=1)}}{P_{B\,(t=0)}}$$

where P_A is the frequency of the dominant lineage and P_B is the frequency of the nondominant lineage before ($t = 0$; juvenile) and after ($t = 1$; adult) a selection episode. Here, we find that individuals of dark purple ancestry are 2.3 times more likely to reach adulthood in the nearshore environment, while those of light purple ancestry are 2.4 times more likely to reach adulthood in the offshore environment. Additionally, only one adult colony with ancestry to either of the two deep lineages (i.e., light or dark green) is found in the shallow sites,

and vice versa from shallow to deep. Juveniles also demonstrate nearly perfect segregation by depth (we found only one juvenile of a shallow lineage at the deep site). To emphasize this pattern of environmental specialization and maintain clarity throughout the remainder of the text, we will refer to the four *M. cavernosa* lineages as follows: Nearshore (dark purple), Offshore (light purple), Deep1 (dark green) and Deep2 (light green) (Figure 1c).

In *S. siderea*, the separation by depth is similarly pronounced among adults but not among juveniles. About half of all juveniles at depth are of dark purple ancestry, which is the most common among shallow adults and entirely dominates the shallow juvenile populations. In fact, we did not find any juveniles of light purple ancestry, the other shallow-exclusive lineage. In such a situation, there is no evidence of specialization between the two shallow lineages across the nearshore and offshore habitats, but again a notable divergence across depth. We will refer to *S. siderea* lineages as follows throughout the remainder of the text: Shallow1 (dark purple), Shallow2 (light purple), Deep1 (dark green) and Deep2 (light green) (Figure 1c).

3.2 | Demographic modelling of lineage pairs

In both species, demographic models that most accurately reproduce pairwise AFS between subpopulations (Figures S5 and S6) all share one important feature. In every case, the model with highest likelihood includes the presence of "islands of differentiation" experiencing lower introgression rates than the rest of the genome, with the best model without this parameter ranking not higher than 20th from the top by the AIC (Figures S7 and S8). Figure 2(a) depicts the proportion of the genome attributable to such islands for each pairwise comparison, and Figure 2(b) provides the fold reduction in introgression rates within the islands compared to the rest of the genome.

In *M. cavernosa*, introgression between lineages within the islands of differentiation is reduced in 18.2%–54.7% of the genome by a factor of 1.1–6.0. Similarly, in *S. siderea*, introgression is reduced in 13.0%–50.9% of the genome by a factor of 2.4–17.7 (Figures 2a,b and 3).

3.3 | Effective population size changes through time

Genetic lineages of both species show broadly similar profiles of effective population size (N_e) through time (Figure 4). In both species, all lineages first show N_e increase between 500 and 200 thousand years ago (ka). After that, three lineages in *M. cavernosa* and one lineage in *S. siderea* experience a reduction around 50–100 ka, followed by re-expansion to about 2.5× the N_e before the reduction. Lastly, two lineages in both *M. cavernosa* and *S. siderea* show decline over the past few thousand years. The ancient and recent expansions with similar time stamps are also inferred by *Moments* models (Figures S5 and S6), although these models do not show population reductions possibly because *Moments* models could only incorporate up to three population size changes. The differences in N_e among lineages are concordant between STAIRWAYPLOT and *Moments* inference.

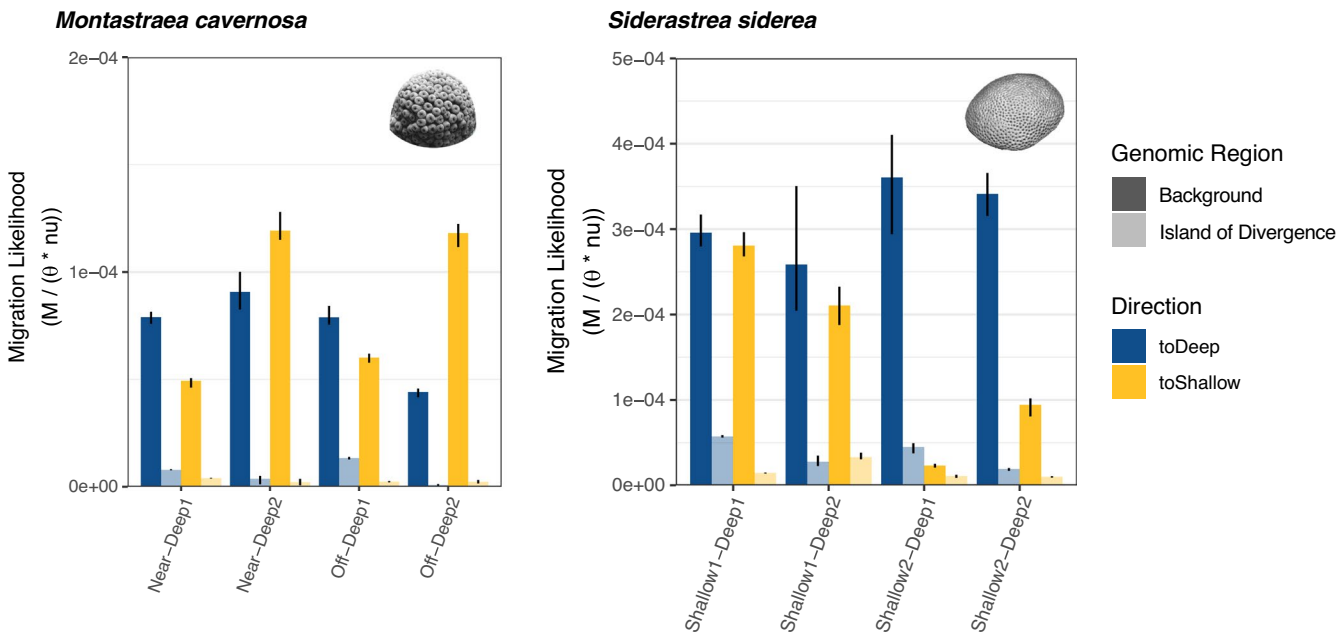

FIGURE 3 Asymmetrical introgression from shallow to deep. Median estimates of asymmetrical migration parameters between shallow and deep lineages output from bootstrapped pairwise demographic modelling for *Montastraea cavernosa* (left) and *Siderastrea siderea* (right). Shallow-to-deep migration estimates are coloured blue and deep-to-shallow estimates are coloured yellow. Colour saturation indicates if the estimate is associated with the background (full colour) or "islands of divergence" (faded) portion of the genome. Error bars depict the lower and upper quartiles of the parameter estimates, based on all bootstrapped modelling runs

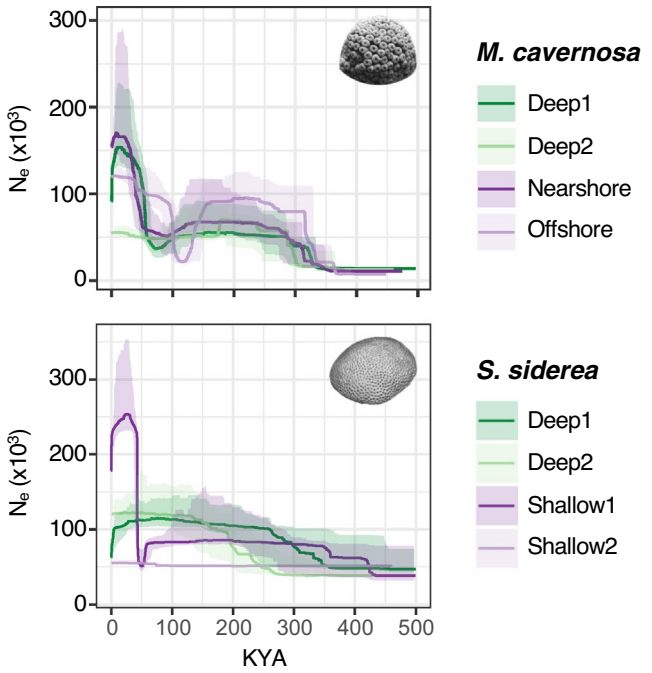

FIGURE 4 Changes in effective population size. History of effective population size changes for each of the four lineages of *Montastraea cavernosa* (top) and *Siderastrea siderea* (bottom), as output from STAIRWAYPLOT. Colours correspond to lineage assignments in Figure 1c. The 75% confidence intervals are displayed as bounding ribbons

In particular, the Shallow2 lineage of *S. siderea* has the smallest N_e both in STAIRWAYPLOT and in *Moments* and even experiences a long-term reduction according to the *Moments* models in every pairwise comparison (Figure S5). Notably, this is the least abundant lineage among our adult samples, and we did not find a single associated juvenile at any site.

3.4 | Loci underlying population structure

The specific loci underlying the distinction between identified lineages were investigated using the novel LD networks methodology, which is an adaptation of the WGCNA to identify groups ("modules") of SNPs that covary across samples. This unsupervised analysis generated exactly four distinct SNP modules for each of the two species, labelled as colours in Figure 5(a). For both species, each of the four SNP module "eigengenes" (i.e., the weighted average genotype of module SNPs) is strongly correlated with each of the four identified lineages (Figure 5b; Figure S9), providing additional support that these lineages reflect the appropriate level of delineation within these species.

To corroborate that the SNP modules comprise loci that underlie the differentiation of each lineage from the others, F_{ST} was calculated for each of the SNPs included in this analysis. In both species, loci with stronger genotype correlation (either positive or negative) to each SNP module eigengene (i.e., stronger membership to each module) also exhibit greater F_{ST} values (*M. cavernosa*: R^2 = 0.24, p < 0.001, *S. siderea*: R^2 = 0.30, p < 0.001; Figure 5c). As expected, the loci identified by BAYESCAN as putatively under selection based on an F_{ST} outlier test fall at the extreme bounds of this association, where the absolute value of SNP–module correlation is less than 0.5 (Figure 6).

Interestingly, module-specific loci do not seem to exhibit any clustering in the genome of *M. cavernosa* (due to the lack of an annotated reference genome, this could not be assessed for *S. siderea*). Instead, these loci seem to be scattered randomly across genomic scaffolds rather than being concentrated in a particular scaffold (Blue: χ^2 = 982.8, df = 1,375, p = 1.0; Brown: χ^2 =1,335.7, df = 1,375, p = 0.77; Turquoise: χ^2 = 652.9, df = 1,375, p = 1.0; Yellow: χ^2 = 1,385.0, df = 1,375, p = 0.42). We also do not find any evidence of functional enrichment among module-forming SNPs based on the GO_MWU analysis (Wright et al., 2015).

4 | DISCUSSION

The data presented here reveal a picture of cryptic genetic structure that follows a strikingly consistent pattern within two widespread coral species of the Florida Keys. In both *Montastraea cavernosa* and *Siderastrea siderea*, genetically distinct lineages exist sympatrically. Both species also exhibit a pattern of environmental specialization, particularly across depth. In *M. cavernosa*, only one individual with ancestry associated with the deep site or either of the shallow sites was found in the opposing environment. In *S. siderea*, nine juvenile colonies associated with shallow ancestry were found at the deep site, but only one adult of the same background was found. No individuals of deep ancestry were found in the shallow habitats. Despite this specialization, we find evidence of ongoing introgression between all pairs of these lineages (Figure 3), as well as putative first-generation hybrids and backcrosses (Figure 1b,c). Notably, introgression is uneven across the genome (Figures 2a,b and 3): between 13% and 54% of the genome experiences several-fold lower introgression rate than the rest, ostensibly due to some form of selection. This unequal introgression across the genome among environmentally specialized lineages is the most notable feature of the genetic system described here.

4.1 | Uneven gene flow across genome

When comparing pairs of genetic lineages, demographic models consistently indicate a substantial portion of the genome exhibits introgression rates that are reduced by a factor of up to 6.0 in *M. cavernosa* and up to 17.7 in *S. siderea* relative to the rest of the genome. Using a novel LD networks approach, we find that covarying SNPs consolidate into distinct lineage-specific modules (Figure 5a,b; Figure S9), where SNPs that exhibit the strongest membership to their respective module also show the highest F_{ST} between lineages (Figure 5c and 6). Notably, there is never an obvious break between

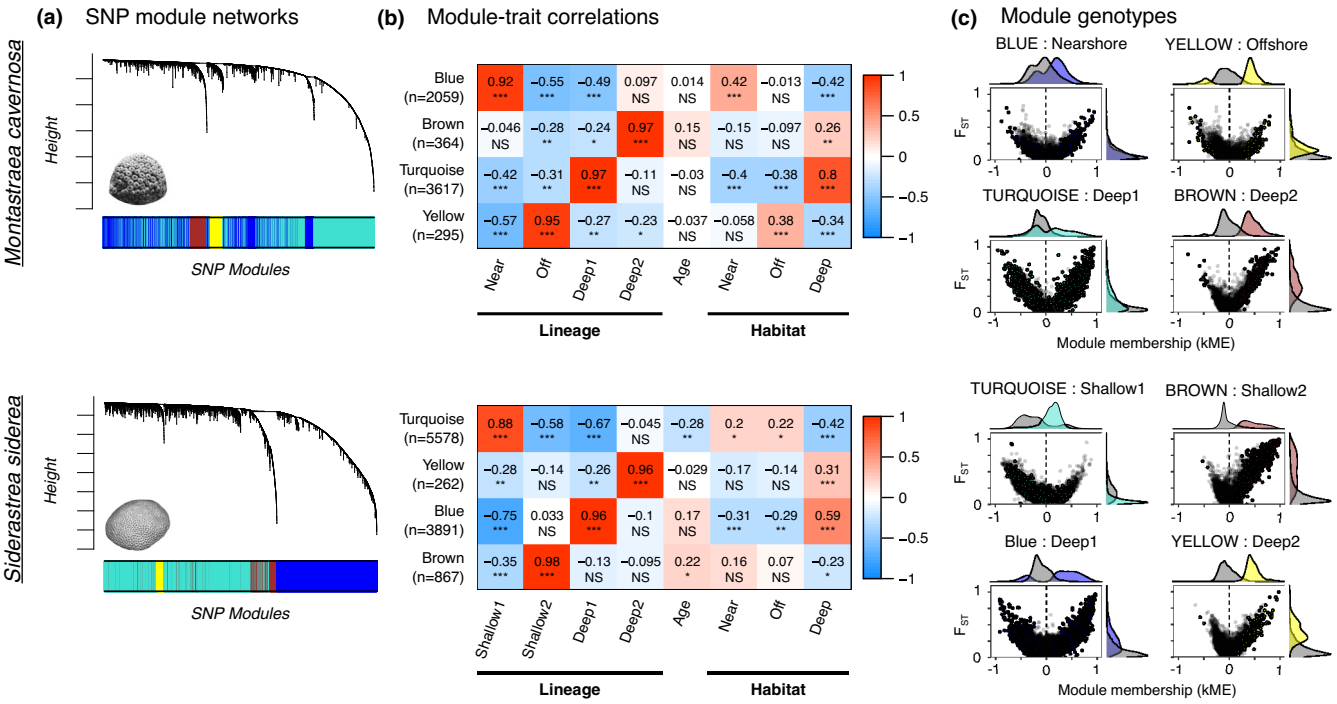

FIGURE 5 SNP modules reflect loci underlying population differentiation. (a) Hierarchical trees display the interconnectedness of loci based on the measure of correlation (R^2). Correlated SNPs are parsed into distinct modules, represented below the trees as colors. (b) SNP module eigengenes, or the weighted average genotype of SNPs within each module, are correlated with sample traits. Correlation coefficients are provided with associated pvalues in parentheses. A positive correlation (red) indicates that the majority of samples positive for the trait had higher derived allele frequency at the loci in the module, while a negative correlation (blue) indicates the opposite. Significance of module-trait correlations are reflected in the intensity of the box fill color and also under the correlation coefficient, as follows: ***$p < 0.0001$, **$p < 0.001$, *$p < 0.05$, NS, not significant. (c) For the four SNP modules (four panels) of each species, SNP module membership is compared to locus-specific pairwise F_{ST} estimates of all lineage pairs that include the lineage most correlated with the SNP module (panel b). SNPs assigned to each module are highlighted in the color corresponding the module name. Density plots along the axes illustrate the tendency for SNPs with highest membership to each module (distance from 0 on the *x*-axis) to also exhibit the highest F_{ST} between the correlated lineage and all other lineages (*y*-axis)

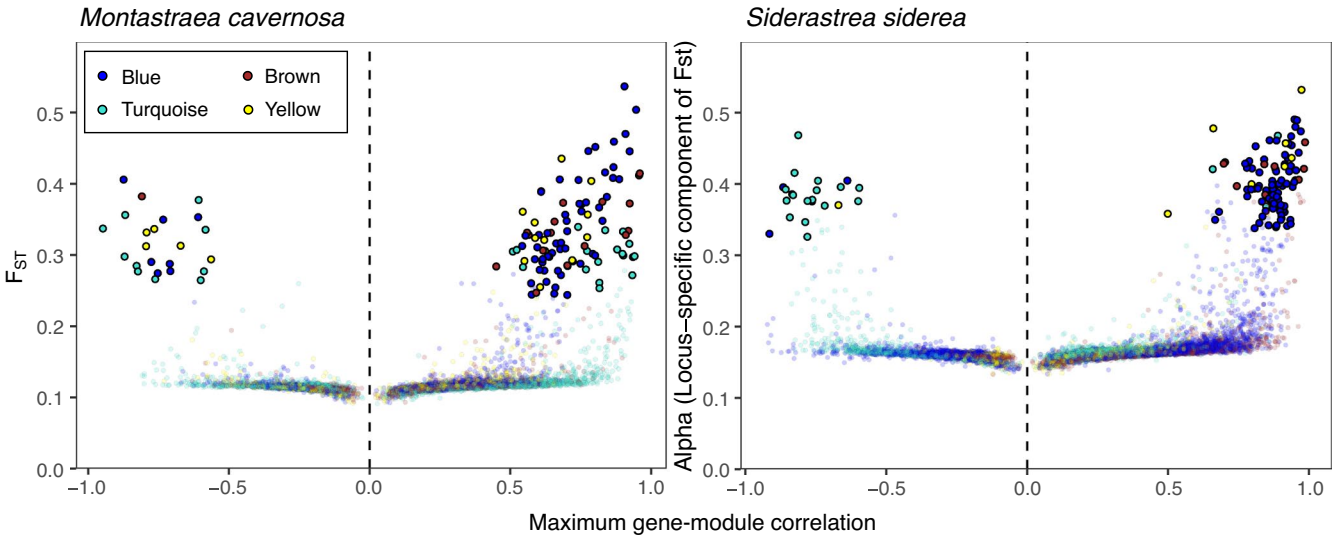

FIGURE 6 SNP module membership recapitulates F_{ST}. Each SNP is represented as a point, coloured based on the WGCNA module to which it is most strongly correlated. Correlation to this module is reflected by its position along the *x*-axis. Positive correlation indicates SNPs that exhibit genotypic changes across samples in the same direction as the module eigengene (i.e., the weighted average genotype of all SNPs in the module). Negative correlation indicates SNPs that exhibit genotypic changes in the opposite direction as the module eigengene. The locus-specific component of F_{ST} between all pairwise lineages, as calculated by BAYESCAN, is reflected on the *y*-axis. SNPs identified as putatively under selection based on an F_{ST} outlier test are in bold

high and low F_{ST} values within each module (Figures 5c and 6), indicating that the distinction between two kinds of loci suggested by our demographic models is just an approximation of the continuum of introgression rates across the genome. Still, the fact that models with heterogeneous introgression fit our data significantly better than models with uniform introgression implies the existence of a mechanism maintaining (or generating) additional genetic differentiation in a substantial portion of the genome.

This pattern of restricted introgression has also been observed in the Caribbean octocoral, *Eunicea flexuosa*, which implies that it may be more common among Anthozoans than is currently recognized (Prada & Hellberg, 2021). The mechanisms underlying such a process can be thought to operate at either the pre- or postzygotic stage. Mechanisms of prezygotic isolation can be diverse, including (in Anthozoa) spawning asynchrony, gametic incompatibility and immigrant inviability (Levitan & Ferrell, 2006; Levitan et al., 2004; Ohki et al., 2015; Prada & Hellberg, 2013). However, all prezygotic mechanisms are expected to generate genome-wide divergence rather than the heterogeneous divergence across the genome.

Rather, postzygotic factors that reduce the fitness of hybrid larvae or adults are a more likely explanation, since this type of incompatibility is expected to be restricted to certain genes rather than the whole genome. One possibility is strong spatially varying selection, preventing introgression of locally adaptive alleles across environmental boundaries. Previous research has shown that fitness-related traits in corals are probably highly polygenic in nature (Fuller et al., 2020; Rose et al., 2018), and may be related to cryptic genetic structure (Gómez-Corrales and Prada, 2020). However, it is difficult to imagine how locally adaptive alleles could be so numerous (more than 50% of the genome in some cases) and how they can be spread evenly across the genome without association to any specific biological functions. Moreover, this explanation clearly does not apply to the sympatric depth-specialized lineages, particularly in *M. cavernosa* where the two deep lineages are the most highly diverged of any lineage pair (Figure 2a). Another, more likely, possibility is that introgression is prevented by intragenomic incompatibility among alleles (Dobzhansky–Muller or DM incompatibilities; Orr, 1996) such that certain combinations of alleles at different loci that arise during lineage mixing are maladaptive and therefore selected against when a first-generation hybrid backcrosses to one of the parental lineages. While the theoretical framework for such a mechanism was first introduced by Dobzhansky (1937) and Muller (1942) over 75 years ago, only recently has genomics research demonstrated empirical support (Powell et al., 2020; reviewed in Presgraves, 2010). The two coral species studied here represent good study systems for future research to investigate the role of DM incompatibilities in creating genetic barriers.

4.2 | Population size changes through time

Inferred N_e values and associated time stamps (Figure 4; Figures S5 and S6) must be viewed with caution because of high uncertainty in the generation time and especially the mutation rate in these corals. Still, fold-change in N_e and relative placement of expansions and declines along the time axis do not depend on these assumptions and can therefore be evaluated more reliably. It is tempting to associate declines around 50–100 ka with glacial cycles and subsequent expansions with the stability of the last interglacial. This inference is similar to the scenario proposed by Prada et al. (2016) with respect to the genus *Orbicella* in the Caribbean basin and Cooke et al. (2020) regarding *Acropora tenuis* in the central Great Barrier Reef. However, this should only be viewed a tentative suggestion given our uncertainty about absolute time. It is also worth mentioning that the "expansion" after 50 ka might not truly be an increase in population size but could instead reflect the onset of introgression between lineages. Such a case would lead to higher genetic diversity and therefore higher N_e within each lineage. The most recent decline in two *M. cavernosa* and two *S. siderea* lineages may appear to reflect the precipitous decline of Florida reefs in the last 50 years (Toth et al., 2019); however, STAIRWAYPLOT is unlikely to resolve such recent events (X. Liu & Fu, 2015). More probably, this N_e decline reflects the longer term decline of Florida Keys reefs since the flooding of the Florida Bay a few thousand years ago (Toth et al., 2018).

4.3 | Environmental specialization across depth

A substantial body of literature investigating vertical connectivity in corals has accumulated in response to renewed interest in the "deep reef refugia" hypothesis. This term refers to the prospect that coral populations at depth, which are protected from the most severe impacts of climate change, may sustain or repopulate degraded shallow reefs through larval subsidy (reviewed in Bongaerts et al., 2010b). However, much of this recent research has revealed a pattern of limited population connectivity across depth. In fact, studies of *M. cavernosa* have demonstrated a strong genetic barrier between deep and shallow populations in the Florida Keys, The Bahamas, U.S. Virgin Islands and Belize (Brazeau et al., 2013; Eckert et al., 2019; Serrano et al., 2014), although not in the NW Gulf of Mexico or Bermuda (Serrano et al., 2014; Studivan & Voss, 2018). Similarly, other species in both the Caribbean and the Indo-Pacific show limited dispersal between depth zones, but with variation between regions and species (Bongaerts et al., 2017; van Oppen et al., 2011; Serrano et al., 2016).

This study provides another example of genetic differentiation across depth, suggesting limited practicality for the "deep reef refugia" hypothesis in the Florida Keys. Furthermore, the notable discrepancy between cross-depth migrants of the juvenile and adult life stages in *S. siderea* offers insight into the mechanism underlying this divergence over a single generation. The presence of juveniles with shallow ancestry at the deep site indicates that successful larval recruitment from shallow to deep sites occurs at an appreciable frequency. However, the lack of adults with the same shallow ancestry implies one of two possibilities. The first and perhaps more likely scenario is that the majority of juveniles are not able to survive the deep

conditions and therefore do not reach adulthood, a straightforward signature of spatially varying selection. This could be due to a number of environmental factors that differ significantly across depth; light availability in particular has been shown to strongly affect coral physiology (Lesser et al., 2010; Suggett et al., 2013; Treignier et al., 2008; Villinski, 2003) and probably plays a role in filtering maladapted genotypes from their non-native habitats. Other selective factors may include temperature conditions, particularly in regions of frequent upwelling, or variations in viable symbiont communities, which are known to be structured significantly by depth (Bongaerts et al., 2015; Eckert et al., 2020; Lesser et al., 2010). Alternatively, because this study represents only a single snapshot of a continuous process, a second possibility is that we have captured a recent shallow-to-deep colonization event in *S. siderea*, which in time may yield a third sustainable adult population at depth.

Moreover, the observed asymmetry of juvenile distribution across depth in *S. siderea*, wherein juveniles of shallow lineage were observed in the deep habitat but not vice versa (Figure 1), mirrors the asymmetry in modelled introgression rates, which tend to be higher from shallow to deep than from deep to shallow (Figure 3). This result is in agreement with that of Bongaerts et al. (2017), where shallow-to-deep introgression in *Agaricia fragilis* is inferred from asymmetry in the private allele distribution, and Prada and Hellberg (2021), where asymmetrical introgression in the Caribbean octocoral *Eunicea flexuosa* is shown to favour the shallow-to-deep to direction. Moreover, it also aligns with recent experimental evidence from two *Stylophora* species and a brooding octocoral demonstrating that shallow-origin larvae exhibit lower settlement specificity across shallow and deep conditions compared with mesophotic-origin larvae (Shlesinger & Loya, 2021).

4.4 | Environmental specialization across reef zones

In addition to the pronounced genetic barrier across depth, there is more subtle evidence of a selection gradient between nearshore and offshore reef zones. Particularly in *M. cavernosa*, comparison of adult and juvenile populations indicates that individuals assigned to the Nearshore or Offshore lineage are more than twice as likely to reach adulthood in their local habitat than the alternative lineage. It is important to note that the fitness calculation used here does not allow for estimation of statistical error; however, previous research on the octocoral *Eunicea flexuosa* shows with greater statistical certainty that differences in the distribution of environment-associated lineages between age groups can be used to infer local adaptation, in this case across a depth and light gradient (Prada & Hellberg, 2014).

Furthermore, this finding from *M. cavernosa* is reflective of previous research demonstrating local adaptation across the cross-shelf gradient, a pattern that is often associated with differences in thermal tolerance. Evidence suggests that corals from nearshore reef habitats, which experience extreme daily and seasonal seawater temperature fluctuations, are more resilient to warming than their outer reef conspecifics, which experience more thermally stable conditions (Barshis et al., 2013; Castillo et al., 2012; Kenkel & Matz, 2016; Palumbi et al., 2014). In the Florida Keys, this pattern is compounded by a cross-shelf gradient in water quality, characterized by decreasing turbidity and nutrient concentrations moving away from shore (Lapointe et al., 2019; Lirman & Fong, 2007). Variation in water quality parameters, such as overall nutrient load, dissolved nutrient stoichiometry and the concentration of suspended particulate matter, can dramatically alter coral physiology (Allgeier et al., 2020; Anthony & Fabricius, 2000; Koop et al., 2001) and have been shown to diminish coral resistance to bleaching and disease (DeCarlo et al., 2020; Vega Thurber et al., 2014; Wiedenmann et al., 2013). It is likely that the combined pressure of these cross-shelf gradients in temperature and water quality conditions is responsible for the observed genetic specialization to each reef zone.

In *S. siderea*, while there is no evidence of a specialization across shallow nearshore and offshore reef zones, it is notable that every pairwise demographic model indicated a recent reduction in effective population size for the Shallow2 lineage (Figure S5). This pattern, coupled with the fact that no juveniles of this lineage were found, suggests that this population may be facing competitive exclusion in this region of the Florida Keys Reef Tract. By contrast, the ubiquity of the larger shallow lineage (Shallow1) across the two shallow sites and evidence of successful recruitment to the deep suggests that this lineage may be capitalizing on a selective advantage throughout this region.

4.5 | Origin of lineages

The fact that two phylogenetically divergent species (belonging to different families of the order Scleractinia) show such strikingly similar patterns of genetic subdivision (Figure 1) and demographic history (Figure 4; Figures S5 and S6) suggests that the mechanism that initially gave rise to their genetic structure might be linked to the properties of the environment that they share (i.e., the Florida Keys Reef Tract). The Florida Keys Reef Tract is unusual among Caribbean reef systems in that it has been influenced by the tidal flow from the Florida Bay over the past few thousand years, which can be detrimental for reef development (Toth et al., 2018). Moreover, it can receive immigrant larvae from distant locations that are not directly connected to each other, such as The Bahamas and Mexico (Schill et al., 2015). It is possible that a combination of these factors led to accumulation and sympatric survival of several distinct lineages that originated elsewhere in the Caribbean.

Overall, we expect that a combination of prezygotic isolation and local adaptation may have played a role in the initial formation of these genetic lineages, and that accumulation of DM incompatibilities during this period of isolation continues to maintain the divergence between lineages despite occurring in sympatry. Interestingly, the *Moments* models indicate a period of isolation for only a subset of the lineage pairs in both species (see Figures S5 and S6 where periods of isolation are depicted as epochs which lack migration

arrows and are highlighted with asterisks), and multiple iterations of this analysis yield slight inconsistencies in the presence or absence of these periods across runs. Thus, these data do not provide conclusive evidence in support or against this hypothesis regarding the origin of lineages, and additional research involving whole-genome sequencing and controlled crosses is needed.

Our data also suggest that new deep lineages tend to originate from shallow rather than from other deep lineages based on the following evidence: (i) the two deep lineages of *M. cavernosa* are the most highly divergent of all lineage pairs in this species (Figure 2a; Table S1), and (ii) in both species the lowest pairwise differentiation involving the Deep2 lineage, both in terms of F_{ST} (Figure 2a) and time since divergence (Figures S5 and S6), occurs with a shallow lineage, not the other deep lineage. Notably, in *M. cavernosa* the closest lineage to Deep2 is the Nearshore lineage, not the Offshore lineage as could have been expected based on physical proximity of the offshore and the deep reef habitats (Figure 1a). Moreover, the Nearshore lineage of *M. cavernosa* is actually the most closely related lineage to the reference genome, despite the reference individual being collected from a near-mesophotic habitat in the Flower Garden Banks (Figure S10). It is possible that the nearshore–deep transition is facilitated by a shared adaptation to lower light conditions, due to higher turbidity nearshore and light attenuation at depth.

4.6 | Broader implications

Before the emergence of stony coral tissue loss disease (SCTLD; Muller et al., 2020; Precht et al., 2016), the two coral species studied here were among the least vulnerable in the Florida Keys (Ruzicka et al., 2013; Toth et al., 2019). Even now, while large adult *M. cavernosa* and *S. siderea* are highly susceptible to SCTLD, young recruits of these species are still numerous and there is optimism for significant recovery. This is in sharp contrast to the once major reef-builders of Caribbean reefs, *Acropora palmata* and *Orbicella* sp., which have largely lost the capacity to replenish their populations through larval recruitment and in the Florida Keys are sustained exclusively by asexual reproduction through fragmentation (van Woesik et al., 2014). It is perhaps not coincidental that these two formerly foundational but now effectively ecologically extinct species are highly genetically uniform in the Florida Keys (Devlin-Durante & Baums, 2017; Manzello et al., 2019), while the two relatively successful species studied here demonstrate similar subdivision into environmentally specialized, semi-isolated genetic lineages. Perhaps the capacity to split and specialize allows the species as a whole to accumulate broader adaptive genetic variation that fuels evolutionary rescue in times of change. This is even more likely considering that despite specialization there is still appreciable gene flow between lineages (Figure 3).

With respect to ongoing coral reef management and restoration efforts, the implication of cryptic diversification and specialization within species is important, as the provenance and genetic background of nursery-propagated corals can inform managers of the most suitable environments for outplanting. In addition, hybridization between lineages *ex situ* might serve the role of assisted gene flow (AGF; Aitken & Whitlock, 2013) by facilitating the flow of adaptive variation across lineage boundaries. Notably, unlike conventional AGF that involves crossing corals from different geographical regions (Baums et al., 2019), such "local AGF" would not be restricted by regulations prohibiting the exchange and breeding of coral genotypes across national borders.

Furthermore, with respect to the expanding research focus on cryptic genetic structure in corals and many other marine and terrestrial taxa, it is worth highlighting that the LD network methodology employed in this study provides the capability to define specific modules of covarying loci underlying this phenomenon. Compared to standard analyses of locus-specific F_{ST}, this approach is well suited to scenarios in which the mechanism of divergence between lineages is polygenic and can be used to resolve correlated allele frequency shifts unique to specific populations. Additionally, although the design of this study limited our ability to associate these loci with clear biological function, we expect the utility of this method to be even greater with higher genomic resolution and when accompanied by phenotypic data, particularly with respect to known fitness-related traits.

ACKNOWLEDGEMENTS

Funding for this work was provided by National Science Foundation award OCE-1737312, and all collections were authorized under Florida Keys National Marine Sanctuaries permit #2015-071. We wish to thank Eric Bartels and Mote's Elizabeth Moore International Center for Coral Reef Research & Restoration for invaluable field assistance and resources. The bioinformatics analysis was accomplished using computational resources provided by the Texas Advanced Computer Center.

AUTHOR CONTRIBUTIONS

M.M. conceived and designed this study. M.M. and G.D. collected tissue samples in the field, and G.D. performed 2bRAD library preparations. Z.F. assembled the *Montastraea cavernosa* reference genome with annotations contributed by Y.L. J.R. and M.M. conducted the bioinformatic and data analysis. J.R. prepared the manuscript with all authors contributing to its final form.

DATA AVAILABILITY STATEMENT

Raw 2bRAD sequence data from this study can be accessed under the NCBI BioProject Accession PRJNA679067. The *Montastraea cavernosa* reference genome is available on the Matz Lab website (https://matzlab.weebly.com/data--code.html). Bioinformatic procedures associated with the *de novo* 2bRAD methodology (https://github.com/z0on/2bRAD_denovo), *Moments*-based demographic modelling (https://github.com/z0on/AFS-analysis-with-moments), LD network analysis (https://github.com/z0on/LDnetworks), and all other data analysis procedures used in this study (https://github.com/jprippe/AdultJuv_Depth_FL) are available in the specified GitHub repositories.

ORCID

John P. Rippe https://orcid.org/0000-0002-6243-0757
Groves Dixon https://orcid.org/0000-0001-5501-6024
Zachary L. Fuller https://orcid.org/0000-0003-4765-9227

REFERENCES

Aitken, S. N., & Whitlock, M. C. (2013). Assisted gene flow to facilitate local adaptation to climate change. *Annual Review of Ecology, Evolution, and Systematics*, *44*(1), 367–388. https://doi.org/10.1146/annurev-ecolsys-110512-135747

Allgeier, J. E., Andskog, M. A., Hensel, E., Appaldo, R., Layman, C., & Kemp, D. W. (2020). Rewiring coral: Anthropogenic nutrients shift diverse coral–symbiont nutrient and carbon interactions toward symbiotic algal dominance. *Global Change Biology*, *26*(10), 5588–5601. https://doi.org/10.1111/gcb.15230

Anthony, K. R. N., & Fabricius, K. E. (2000). Shifting roles of heterotrophy and autotrophy in coral energetics under varying turbidity. *Journal of Experimental Marine Biology and Ecology*, *252*(2), 221–253. https://doi.org/10.1016/S0022-0981(00)00237-9

Aranda, M., Li, Y., Liew, Y. J., Baumgarten, S., Simakov, O., Wilson, M. C., Piel, J., Ashoor, H., Bougouffa, S., Bajic, V. B., Ryu, T., Ravasi, T., Bayer, T., Micklem, G., Kim, H., Bhak, J., LaJeunesse, T. C., & Voolstra, C. R. (2016). Genomes of coral dinoflagellate symbionts highlight evolutionary adaptations conducive to a symbiotic lifestyle. *Scientific Reports*, *6*(1), 39734. https://doi.org/10.1038/srep39734

Barkley, H. C., Cohen, A. L., McCorkle, D. C., & Golbuu, Y. (2017). Mechanisms and thresholds for pH tolerance in Palau corals. *Journal of Experimental Marine Biology and Ecology*, *489*, 7–14. https://doi.org/10.1016/j.jembe.2017.01.003

Barshis, D. J., Ladner, J. T., Oliver, T. A., Seneca, F. O., Traylor-Knowles, N., & Palumbi, S. R. (2013). Genomic basis for coral resilience to climate change. *Proceedings of the National Academy of Sciences*, *110*(4), 1387–1392. https://doi.org/10.1073/pnas.1210224110

Baums, I. B., Baker, A. C., Davies, S. W., Grottoli, A. G., Kenkel, C. D., Kitchen, S. A., Kuffner, I. B., LaJeunesse, T. C., Matz, M. V., Miller, M. W., Parkinson, J. E., & Shantz, A. A. (2019). Considerations for maximizing the adaptive potential of restored coral populations in the western Atlantic. *Ecological Applications*, *29*(8), e01978. https://doi.org/10.1002/eap.1978

Bongaerts, P., Frade, P. R., Hay, K. B., Englebert, N., Latijnhouwers, K. R. W., Bak, R. P. M., Vermeij, M. J. A., & Hoegh-Guldberg, O. (2015). Deep down on a Caribbean reef: Lower mesophotic depths harbor a specialized coral-endosymbiont community. *Scientific Reports*, *5*(1), 7652. https://doi.org/10.1038/srep07652

Bongaerts, P., Ridgway, T., Sampayo, E. M., & Hoegh-Guldberg, O. (2010b). Assessing the 'deep reef refugia' hypothesis: Focus on Caribbean reefs. *Coral Reefs*, *29*(2), 309–327. https://doi.org/10.1007/s00338-009-0581-x

Bongaerts, P., Riginos, C., Brunner, R., Englebert, N., Smith, S. R., & Hoegh-Guldberg, O. (2017). Deep reefs are not universal refuges: Reseeding potential varies among coral species. *Science Advances*, *3*(2), e1602373. https://doi.org/10.1126/sciadv.1602373

Bongaerts, P., Riginos, C., Ridgway, T., Sampayo, E. M., van Oppen, M. J. H., Englebert, N., Vermeulen, F., & Hoegh-Guldberg, O. (2010a). Genetic divergence across habitats in the widespread coral seriatopora hystrix and its associated symbiodinium. *PLoS One*, *5*(5), e10871. https://doi.org/10.1371/journal.pone.0010871

Brazeau, D. A., Lesser, M. P., & Slattery, M. (2013). Genetic structure in the coral, *Montastraea cavernosa*: assessing genetic differentiation among and within mesophotic reefs. *PLoS One*, *8*(5), https://doi.org/10.1371/journal.pone.0065845

Burnham, K. P., & Anderson, D. R. (2002). *Model selection and multimodel inference: A practical information-theoretic approach* (2nd ed.). Springer-Verlag. https://doi.org/10.1007/b97636

Castillo, K. D., Ries, J. B., Weiss, J. M., & Lima, F. P. (2012). Decline of forereef corals in response to recent warming linked to history of thermal exposure. *Nature Climate Change*, *2*(10), 756–760. https://doi.org/10.1038/nclimate1577

Cooke, I., Ying, H., Forêt, S., Bongaerts, P., Strugnell, J. M., Simakov, O., Zhang, J., Field, M. A., Rodriguez-Lanetty, M., Bell, S. C., Bourne, D. G., van Oppen, M. J., Ragan, M. A., & Miller, D. J. (2020). Genomic signatures in the coral holobiont reveal host adaptations driven by Holocene climate change and reef specific symbionts. *Science Advances*, *6*(48), eabc6318. https://doi.org/10.1126/sciadv.abc6318

DeCarlo, T. M., Gajdzik, L., Ellis, J., Coker, D. J., Roberts, M. B., Hammerman, N. M., Pandolfi, J. M., Monroe, A. A., & Berumen, M. L. (2020). Nutrient-supplying ocean currents modulate coral bleaching susceptibility. *Science Advances*, *6*(34), eabc5493. https://doi.org/10.1126/sciadv.abc5493

Devlin-Durante, M. K., & Baums, I. B. (2017). Genome-wide survey of single-nucleotide polymorphisms reveals fine-scale population structure and signs of selection in the threatened Caribbean elkhorn coral, *Acropora palmata*. *PeerJ*, *5*, e4077. https://doi.org/10.7717/peerj.4077

Dixon, G. B., Davies, S. W., Aglyamova, G. V., Meyer, E., Bay, L. K., & Matz, M. V. (2015). Genomic determinants of coral heat tolerance across latitudes. *Science*, *348*(6242), 1460–1462. https://doi.org/10.1126/science.1261224

Dobzhansky, T. (1937). *Genetics and the Origin of species*. Columbia University Press.

Dougan, K. (2020). *A comparative genomics exploration of inter-partner metabolic signaling in the coral-algal symbiosis [PhD Dissertation]*. FIU Electronic Theses and Dissertations.

Duranton, M., Allal, F., Fraïsse, C., Bierne, N., Bonhomme, F., & Gagnaire, P.-A. (2018). The origin and remolding of genomic islands of differentiation in the European sea bass. *Nature Communications*, *9*(1), 2518. https://doi.org/10.1038/s41467-018-04963-6

Eckert, R. J., Reaume, A. M., Sturm, A. B., Studivan, M. S., & Voss, J. D. (2020). Depth influences symbiodiniaceae associations among *Montastraea cavernosa* corals on the Belize barrier reef. *Frontiers in Microbiology*, *11*, 518. https://doi.org/10.3389/fmicb.2020.00518

Eckert, R. J., Studivan, M. S., & Voss, J. D. (2019). Populations of the coral species *Montastraea cavernosa* on the Belize Barrier Reef lack vertical connectivity. *Scientific Reports*, *9*(1), 7200. https://doi.org/10.1038/s41598-019-43479-x

Foll, M., & Gaggiotti, O. (2008). A genome-scan method to identify selected loci appropriate for both dominant and codominant markers: A Bayesian perspective. *Genetics*, *180*(2), 977–993. https://doi.org/10.1534/genetics.108.092221

Fox, E. A., Wright, A. E., Fumagalli, M., & Vieira, F. G. (2019). ngsLD: Evaluating linkage disequilibrium using genotype likelihoods. *Bioinformatics*, *35*(19), 3855–3856. https://doi.org/10.1093/bioinformatics/btz200

Fu, L., Niu, B., Zhu, Z., Wu, S., & Li, W. (2012). CD-HIT: Accelerated for clustering the next-generation sequencing data. *Bioinformatics*, *28*(23), 3150–3152. https://doi.org/10.1093/bioinformatics/bts565

Fuller, Z. L., Mocellin, V. J. L., Morris, L. A., Cantin, N., Shepherd, J., Sarre, L., Peng, J., Liao, Y., Pickrell, J., Andolfatto, P., Matz, M., Bay, L. K., & Przeworski, M. (2020). Population genetics of the coral *Acropora millepora*: Toward genomic prediction of bleaching. *Science*, *369*(6501), https://doi.org/10.1126/science.aba4674

Gómez-Corrales, M., & Prada, C. (2020). Cryptic lineages respond differently to coral bleaching. *Molecular Ecology*, *29*(22), 4265–4273. https://doi.org/10.1111/mec.15631

Gravel, S. (n.d.). *Moments: Tools for demographic inference [BitBucket Repository]*. Retrieved from https://bitbucket.org/simongravel/moments/src/master/

Hagedorn, M., Page, C. A., O'Neil, K., Flores, D. M., Tichy, L., Chamberland, V. F., Lager, C., Zuchowicz, N., Lohr, K., Blackburn,

H., Vardi, T., Moore, J., Moore, T., Vermeij, M. J. A., & Marhaver, K. L. (2018). *Successful demonstration of assisted gene flow in the threatened coral Acropora Palmata across genetically-isolated caribbean populations using cryopreserved sperm*. BioRxiv, 492447, https://doi.org/10.1101/492447

Hoegh-Guldberg, O., Mumby, P. J., Hooten, A. J., Steneck, R. S., Greenfield, P., Gomez, E., Harvell, C. D., Sale, P. F., Edwards, A. J., Caldeira, K., Knowlton, N., Eakin, C. M., Iglesias-Prieto, R., Muthiga, N., Bradbury, R. H., Dubi, A., & Hatziolos, M. E. (2007). Coral reefs under rapid climate change and ocean acidification. *Science*, *318*(5857), 1737–1742. https://doi.org/10.1126/science.1152509

Howells, E. J., Berkelmans, R., van Oppen, M. J. H., Willis, B. L., & Bay, L. K. (2013). Historical thermal regimes define limits to coral acclimatization. *Ecology*, *94*(5), 1078–1088. https://doi.org/10.1890/12-1257.1

Hughes, T. P., Barnes, M. L., Bellwood, D. R., Cinner, J. E., Cumming, G. S., Jackson, J. B. C., Kleypas, J., van de Leemput, I. A., Lough, J. M., Morrison, T. H., Palumbi, S. R., van Nes, E. H., & Scheffer, M. (2017). Coral reefs in the anthropocene. *Nature*, *546*(7656), 82–90. https://doi.org/10.1038/nature22901

Jouganous, J., Long, W., Ragsdale, A. P., & Gravel, S. (2017). Inferring the joint demographic history of multiple populations: Beyond the diffusion approximation. *Genetics*, *206*(3), 1549–1567. https://doi.org/10.1534/genetics.117.200493

Kenkel, C. D., Almanza, A. T., & Matz, M. V. (2015). Fine-scale environmental specialization of reef-building corals might be limiting reef recovery in the Florida Keys. *Ecology*, *96*(12), 3197–3212. https://doi.org/10.1890/14-2297.1

Kenkel, C. D., Goodbody-Gringley, G., Caillaud, D., Davies, S. W., Bartels, E., & Matz, M. V. (2013). Evidence for a host role in thermotolerance divergence between populations of the mustard hill coral (*Porites astreoides*) from different reef environments. *Molecular Ecology*, *22*(16), 4335–4348. https://doi.org/10.1111/mec.12391

Kenkel, C. D., & Matz, M. V. (2016). Gene expression plasticity as a mechanism of coral adaptation to a variable environment. *Nature Ecology & Evolution*, *1*(1), 1–6. https://doi.org/10.1038/s41559-016-0014

Kim, S. Y., Lohmueller, K. E., Albrechtsen, A., Li, Y., Korneliussen, T., Tian, G., Grarup, N., Jiang, T., Andersen, G., Witte, D., Jorgensen, T., Hansen, T., Pedersen, O., Wang, J., & Nielsen, R. (2011). Estimation of allele frequency and association mapping using next-generation sequencing data. *BMC Bioinformatics*, *12*(1), 231. https://doi.org/10.1186/1471-2105-12-231

Koop, K., Booth, D., Broadbent, A., Brodie, J., Bucher, D., Capone, D., Coll, J., Dennison, W., Erdmann, M., Harrison, P., Hoegh-Guldberg, O., Hutchings, P., Jones, Gb, Larkum, A. W. D., O'Neil, J., Steven, A., Tentori, E., Ward, S., Williamson, J., & Yellowlees, D. (2001). ENCORE: The effect of nutrient enrichment on coral reefs. Synthesis of results and conclusions. *Marine Pollution Bulletin*, *42*(2), 91–120. https://doi.org/10.1016/S0025-326X(00)00181-8

Korneliussen, T. S., Albrechtsen, A., & Nielsen, R. (2014). ANGSD: Analysis of next generation sequencing data. *BMC Bioinformatics*, *15*(1), 356. https://doi.org/10.1186/s12859-014-0356-4

Ladner, J. T., & Palumbi, S. R. (2012). Extensive sympatry, cryptic diversity and introgression throughout the geographic distribution of two coral species complexes. *Molecular Ecology*, *21*(9), 2224–2238. https://doi.org/10.1111/j.1365-294X.2012.05528.x

Langfelder, P., & Horvath, S. (2008). WGCNA: An R package for weighted correlation network analysis. *BMC Bioinformatics*, *9*(1), 559. https://doi.org/10.1186/1471-2105-9-559

Langmead, B., & Salzberg, S. L. (2012). Fast gapped-read alignment with Bowtie 2. *Nature Methods*, *9*(4), 357–359. https://doi.org/10.1038/nmeth.1923

Lapointe, B. E., Brewton, R. A., Herren, L. W., Porter, J. W., & Hu, C. (2019). Nitrogen enrichment, altered stoichiometry, and coral reef decline at Looe Key, Florida Keys, USA: A 3-decade study. *Marine Biology*, *166*(8), 108. https://doi.org/10.1007/s00227-019-3538-9

Lesser, M. P. (2000). Depth-dependent photoacclimatization to solar ultraviolet radiation in the Caribbean coral *Montastraea faveolata*. *Marine Ecology Progress Series*, *192*, 137–151. https://doi.org/10.3354/meps192137

Lesser, M. P., Slattery, M., Stat, M., Ojimi, M., Gates, R. D., & Grottoli, A. (2010). Photoacclimatization by the coral *Montastraea cavernosa* in the mesophotic zone: Light, food, and genetics. *Ecology*, *91*(4), 990–1003. https://doi.org/10.1890/09-0313.1

Levitan, D. R., & Ferrell, D. L. (2006). Selection on gamete recognition proteins depends on sex, density, and genotype frequency. *Science*, *312*(5771), 267–269. https://doi.org/10.1126/science.1122183

Levitan, D. R., Fukami, H., Jara, J., Kline, D., McGovern, T. M., McGhee, K. E., Swanson, C. A., & Knowlton, N. (2004). Mechanisms of reproductive isolation among sympatric broadcast-spawning corals of the *Montastraea Annularis* species complex. *Evolution*, *58*(2), 308–323. https://doi.org/10.1111/j.0014-3820.2004.tb01647.x

Li, H., Handsaker, B., Wysoker, A., Fennell, T., Ruan, J., Homer, N., Marth, G., Abecasis, G., Durbin, R, & 1000 Genome Project Data Processing Subgroup. (2009). The sequence alignment/map format and SAMtools. *Bioinformatics (Oxford, England)*, *25*(16), 2078–2079. https://doi.org/10.1093/bioinformatics/btp352

Li, H., & Ralph, P. (2019). Local PCA shows how the effect of population structure differs along the genome. *Genetics*, *211*(1), 289–304. https://doi.org/10.1534/genetics.118.301747

Lirman, D., & Fong, P. (2007). Is proximity to land-based sources of coral stressors an appropriate measure of risk to coral reefs? An example from the Florida Reef Tract. *Marine Pollution Bulletin*, *54*(6), 779–791. https://doi.org/10.1016/j.marpolbul.2006.12.014

Liu, H., Stephens, T. G., González-Pech, R. A., Beltran, V. H., Lapeyre, B., Bongaerts, P., Cooke, I., Aranda, M., Bourne, D. G., Forêt, S., Miller, D. J., van Oppen, M. J. H., Voolstra, C. R., Ragan, M. A., & Chan, C. X. (2018). Symbiodinium genomes reveal adaptive evolution of functions related to coral-dinoflagellate symbiosis. *Communications Biology*, *1*(1), 1–11. https://doi.org/10.1038/s42003-018-0098-3

Liu, X., & Fu, Y.-X. (2015). Exploring population size changes using SNP frequency spectra. *Nature Genetics*, *47*(5), 555–559. https://doi.org/10.1038/ng.3254

Manzello, D. P., Matz, M. V., Enochs, I. C., Valentino, L., Carlton, R. D., Kolodziej, G., Serrano, X., Towle, E. K., & Jankulak, M. (2019). Role of host genetics and heat-tolerant algal symbionts in sustaining populations of the endangered coral *Orbicella faveolata* in the Florida Keys with ocean warming. *Global Change Biology*, *25*(3), 1016–1031. https://doi.org/10.1111/gcb.14545

Martin, M. (2011). Cutadapt removes adapter sequences from high-throughput sequencing reads. *EMBnet.Journal*, *17*(1), 10–12. https://doi.org/10.14806/ej.17.1.200

Matz, M. V. (2018). Fantastic beasts and how to sequence them: Ecological genomics for obscure model organisms. *Trends in Genetics*, *34*(2), 121–132. https://doi.org/10.1016/j.tig.2017.11.002

Matz, M. V., Treml, E. A., Aglyamova, G. V., & Bay, L. K. (2018). Potential and limits for rapid genetic adaptation to warming in a Great Barrier Reef coral. *PLoS Genetics*, *14*(4), e1007220. https://doi.org/10.1371/journal.pgen.1007220

Meisner, J., & Albrechtsen, A. (2018). Inferring population structure and admixture proportions in low-depth NGS data. *Genetics*, *210*(2), 719–731. https://doi.org/10.1534/genetics.118.301336

Muller, E. M., Sartor, C., Alcaraz, N. I., & van Woesik, R. (2020). Spatial epidemiology of the stony-coral-tissue-loss disease in Florida. *Frontiers in Marine Science*, *7*, 163. https://doi.org/10.3389/fmars.2020.00163

Muller, H. J. (1942). Isolating mechanisms, evolution, and temperature. *Biological Symposia*, *6*, 71–125.

Nielsen, R., Korneliussen, T., Albrechtsen, A., Li, Y., & Wang, J. (2012). SNP calling, genotype calling, and sample allele frequency estimation from new-generation sequencing data. *PLoS One*, *7*(7), e37558. https://doi.org/10.1371/journal.pone.0037558

Ohki, S., Kowalski, R. K., Kitanobo, S., & Morita, M. (2015). Changes in spawning time led to the speciation of the broadcast spawning corals Acropora digitifera and the cryptic species *Acropora* sp. 1 with similar gamete recognition systems. *Coral Reefs*, *34*(4), 1189–1198. https://doi.org/10.1007/s00338-015-1337-4

Oksanen, J., Blanchet, F. G., Friendly, M., Kindt, R., Legendre, P., McGlinn, D., Minchin, P. R., O'Hara, R. B., Simpson, G. L., Solymos, P., Stevens, M. H. H., Szoecs, E., & Wagner, H. (2019). *vegan: Community Ecology Package*. https://CRAN.R-project.org/package=vegan

Orr, H. A. (1996). Dobzhansky, bateson, and the genetics of speciation. *Genetics*, *144*(4), 1331–1335.

Palumbi, S. R. (2004). Marine reserves and ocean neighborhoods: The spatial scale of marine populations and their management. *Annual Review of Environment and Resources*, *29*(1), 31–68. https://doi.org/10.1146/annurev.energy.29.062403.102254

Palumbi, S. R., Barshis, D. J., Traylor-Knowles, N., & Bay, R. A. (2014). Mechanisms of reef coral resistance to future climate change. *Science*, *344*(6186), 895–898. https://doi.org/10.1126/science.1251336.

Powell, D. L., García-Olazábal, M., Keegan, M., Reilly, P., Du, K., Díaz-Loyo, A. P., Banerjee, S., Blakkan, D., Reich, D., Andolfatto, P., Rosenthal, G. G., Schartl, M., & Schumer, M. (2020). Natural hybridization reveals incompatible alleles that cause melanoma in swordtail fish. *Science*, *368*(6492), 731–736. https://doi.org/10.1126/science.aba5216

Prada, C., Hanna, B., Budd, A. F., Woodley, C. M., Schmutz, J., Grimwood, J., Iglesias-Prieto, R., Pandolfi, J. M., Levitan, D., Johnson, K. G., Knowlton, N., Kitano, H., DeGiorgio, M., & Medina, M. (2016). Empty niches after extinctions increase population sizes of modern corals. *Current Biology*, *26*(23), 3190–3194. https://doi.org/10.1016/j.cub.2016.09.039

Prada, C., & Hellberg, M. E. (2013). Long prereproductive selection and divergence by depth in a Caribbean candelabrum coral. *Proceedings of the National Academy of Sciences*, *110*(10), 3961–3966. https://doi.org/10.1073/pnas.1208931110

Prada, C., & Hellberg, M. E. (2014). Strong natural selection on juveniles maintains a narrow adult hybrid zone in a broadcast spawner. *The American Naturalist*, *184*(6), 702–713. https://doi.org/10.1086/678403

Prada, C., & Hellberg, M. E. (2021). Speciation-by-depth on coral reefs: Sympatric divergence with gene flow or cryptic transient isolation? *Journal of Evolutionary Biology*, *34*(1), 128–137. https://doi.org/10.1111/jeb.13731

Precht, W. F., Gintert, B. E., Robbart, M. L., Fura, R., & van Woesik, R. (2016). unprecedented disease-related coral mortality in southeastern Florida. *Scientific Reports*, *6*(1), 31374. https://doi.org/10.1038/srep31374

Presgraves, D. C. (2010). The molecular evolutionary basis of species formation. *Nature Reviews Genetics*, *11*(3), 175–180. https://doi.org/10.1038/nrg2718

Quigley, K. M., Bay, L. K., & van Oppen, M. J. H. (2019). The active spread of adaptive variation for reef resilience. *Ecology and Evolution*, *9*(19), 11122–11135. https://doi.org/10.1002/ece3.5616

R Core Team. (2019). *R: A language and environment for statistical computing*. R Foundation for Statistical Computing. https://www.R-project.org/

Richards, Z. T., Berry, O., & van Oppen, M. J. H. (2016). Cryptic genetic divergence within threatened species of Acropora coral from the Indian and Pacific Oceans. *Conservation Genetics*, *17*(3), 577–591. https://doi.org/10.1007/s10592-015-0807-0

Richards, Z. T., Miller, D. J., & Wallace, C. C. (2013). Molecular phylogenetics of geographically restricted Acropora species: Implications for threatened species conservation. *Molecular Phylogenetics and Evolution*, *69*(3), 837–851. https://doi.org/10.1016/j.ympev.2013.06.020

Ronce, O., & Kirkpatrick, M. (2001). When sources become sinks: Migrational meltdown in heterogeneous habitats. *Evolution*, *55*(8), 1520–1531. https://doi.org/10.1111/j.0014-3820.2001.tb00672.x

Rose, N. H., Bay, R. A., Morikawa, M. K., & Palumbi, S. R. (2018). Polygenic evolution drives species divergence and climate adaptation in corals. *Evolution*, *72*(1), 82–94. https://doi.org/10.1111/evo.13385

Rosser, N. L. (2015). Asynchronous spawning in sympatric populations of a hard coral reveals cryptic species and ancient genetic lineages. *Molecular Ecology*, *24*(19), 5006–5019. https://doi.org/10.1111/mec.13372

Ruzicka, R. R., Colella, M. A., Porter, J. W., Morrison, J. M., Kidney, J. A., Brinkhuis, V., Lunz, K. S., Macaulay, K. A., Bartlett, L. A., Meyers, M. K., & Colee, J. (2013). Temporal changes in benthic assemblages on Florida Keys reefs 11 years after the 1997/1998 El Niño. *Marine Ecology Progress Series*, *489*, 125–141. https://doi.org/10.3354/meps10427

Schill, S. R., Raber, G. T., Roberts, J. J., Treml, E. A., Brenner, J., & Halpin, P. N. (2015). No reef is an island: Integrating coral reef connectivity data into the design of regional-scale marine protected area networks. *PLoS One*, *10*(12), e0144199. https://doi.org/10.1371/journal.pone.0144199

Schmidt-Roach, S., Lundgren, P., Miller, K. J., Gerlach, G., Noreen, A. M. E., & Andreakis, N. (2013). Assessing hidden species diversity in the coral *Pocillopora damicornis* from Eastern Australia. *Coral Reefs*, *32*(1), 161–172. https://doi.org/10.1007/s00338-012-0959-z

Serrano, X., Baums, I. B., O'Reilly, K., Smith, T. B., Jones, R. J., Shearer, T. L., Nunes, F. L. D., & Baker, A. C. (2014). Geographic differences in vertical connectivity in the Caribbean coral *Montastraea cavernosa* despite high levels of horizontal connectivity at shallow depths. *Molecular Ecology*, *23*(17), 4226–4240. https://doi.org/10.1111/mec.12861

Serrano, X., Baums, I. B., Smith, T. B., Jones, R. J., Shearer, T. L., & Baker, A. C. (2016). Long distance dispersal and vertical gene flow in the Caribbean brooding coral *Porites astreoides*. *Scientific Reports*, *6*(1), 21619. https://doi.org/10.1038/srep21619

Shlesinger, T., & Loya, Y. (2021). Depth-dependent parental effects create invisible barriers to coral dispersal. *Communications Biology*, *4*(1), 1–10. https://doi.org/10.1038/s42003-021-01727-9

Shoguchi, E., Shinzato, C., Kawashima, T., Gyoja, F., Mungpakdee, S., Koyanagi, R., Takeuchi, T., Hisata, K., Tanaka, M., Fujiwara, M., Hamada, M., Seidi, A., Fujie, M., Usami, T., Goto, H., Yamasaki, S., Arakaki, N., Suzuki, Y., Sugano, S., … Satoh, N. (2013). Draft assembly of the *Symbiodinium minutum* nuclear genome reveals dinoflagellate gene structure. *Current Biology*, *23*(15), 1399–1408. https://doi.org/10.1016/j.cub.2013.05.062

Skotte, L., Korneliussen, T. S., & Albrechtsen, A. (2013). Estimating individual admixture proportions from next generation sequencing data. *Genetics*, *195*(3), 693–702. https://doi.org/10.1534/genetics.113.154138

Studivan, M. S., & Voss, J. D. (2018). Population connectivity among shallow and mesophotic *Montastraea cavernosa* corals in the Gulf of Mexico identifies potential for refugia. *Coral Reefs*, *37*(4), 1183–1196. https://doi.org/10.1007/s00338-018-1733-7

Suggett, D. J., Dong, L. F., Lawson, T., Lawrenz, E., Torres, L., & Smith, D. J. (2013). Light availability determines susceptibility of reef building corals to ocean acidification. *Coral Reefs*, *32*(2), 327–337. https://doi.org/10.1007/s00338-012-0996-7

Toth, L. T., Kuffner, I. B., Stathakopoulos, A., & Shinn, E. A. (2018). A 3,000-year lag between the geological and ecological shutdown of Florida's coral reefs. *Global Change Biology*, *24*(11), 5471–5483. https://doi.org/10.1111/gcb.14389

Toth, L. T., Stathakopoulos, A., Kuffner, I. B., Ruzicka, R. R., Colella, M. A., & Shinn, E. A. (2019). The unprecedented loss of Florida's reef-building corals and the emergence of a novel coral-reef assemblage. *Ecology*, *100*(9), e02781. https://doi.org/10.1002/ecy.2781

Treignier, C., Grover, R., Ferrier-Pagés, C., & Tolosa, I. (2008). Effect of light and feeding on the fatty acid and sterol composition of zooxanthellae and host tissue isolated from the scleractinian coral *Turbinaria reniformis*. *Limnology and Oceanography*, *53*(6), 2702–2710. https://doi.org/10.4319/lo.2008.53.6.2702

van Oppen, M. J. H., Bongaerts, P., Underwood, J. N., Peplow, L. M., & Cooper, T. F. (2011). The role of deep reefs in shallow reef recovery: An assessment of vertical connectivity in a brooding coral from west and east Australia. *Molecular Ecology*, *20*(8), 1647–1660. https://doi.org/10.1111/j.1365-294X.2011.05050.x

van Oppen, M. J. H., Gates, R. D., Blackall, L. L., Cantin, N., Chakravarti, L. J., Chan, W. Y., Cormick, C., Crean, A., Damjanovic, K., Epstein, H., Harrison, P. L., Jones, T. A., Miller, M., Pears, R. J., Peplow, L. M., Raftos, D. A., Schaffelke, B., Stewart, K., Torda, G., … Putnam, H. M. (2017). Shifting paradigms in restoration of the world's coral reefs. *Global Change Biology*, *23*(9), 3437–3448. https://doi.org/10.1111/gcb.13647

van Oppen, M. J. H., Oliver, J. K., Putnam, H. M., & Gates, R. D. (2015). Building coral reef resilience through assisted evolution. *Proceedings of the National Academy of Sciences*, *112*(8), 2307–2313. https://doi.org/10.1073/pnas.1422301112

van Woesik, R., Scott, W. J., & Aronson, R. B. (2014). Lost opportunities: Coral recruitment does not translate to reef recovery in the Florida Keys. *Marine Pollution Bulletin*, *88*(1), 110–117. https://doi.org/10.1016/j.marpolbul.2014.09.017

Vega Thurber, R. L., Burkepile, D. E., Fuchs, C., Shantz, A. A., McMinds, R., & Zaneveld, J. R. (2014). Chronic nutrient enrichment increases prevalence and severity of coral disease and bleaching. *Global Change Biology*, *20*(2), 544–554. https://doi.org/10.1111/gcb.12450

Villinski, J. T. (2003). Depth-independent reproductive characteristics for the Caribbean reef-building coral *Montastraea faveolata*. *Marine Biology*, *142*(6), 1043–1053. https://doi.org/10.1007/s00227-002-0997-0

Vollmer, S. V., & Palumbi, S. R. (2002). Hybridization and the evolution of reef coral diversity. *Science*, *296*(5575), 2023–2025. https://doi.org/10.1126/science.1069524

Wang, S., Meyer, E., McKay, J. K., & Matz, M. V. (2012). 2b-RAD: A simple and flexible method for genome-wide genotyping. *Nature Methods*, *9*(8), 808–810. https://doi.org/10.1038/nmeth.2023

Warner, P. A., van Oppen, M. J. H., & Willis, B. L. (2015). Unexpected cryptic species diversity in the widespread coral Seriatopora hystrix masks spatial-genetic patterns of connectivity. *Molecular Ecology*, *24*(12), 2993–3008. https://doi.org/10.1111/mec.13225

Wiedenmann, J., D'Angelo, C., Smith, E. G., Hunt, A. N., Legiret, F.-E., Postle, A. D., & Achterberg, E. P. (2013). Nutrient enrichment can increase the susceptibility of reef corals to bleaching. *Nature Climate Change*, *3*(2), 160–164. https://doi.org/10.1038/nclimate1661

Willis, B. L., Babcock, R. C., Harrison, P. L., & Wallace, C. C. (1997). Experimental hybridization and breeding incompatibilities within the mating systems of mass spawning reef corals. *Coral Reefs*, *16*, S53–S65. https://doi.org/10.1007/s003380050242

Willis, B. L., van Oppen, M. J. H., Miller, D. J., Vollmer, S. V., & Ayre, D. J. (2006). The role of hybridization in the evolution of reef corals. *Annual Review of Ecology, Evolution, and Systematics*, *37*(1), 489–517. https://doi.org/10.1146/annurev.ecolsys.37.091305.110136

Wright, R. M., Aglyamova, G. V., Meyer, E., & Matz, M. V. (2015). Gene expression associated with white syndromes in a reef building coral. *Acropora hyacinthus*. *BMC Genomics*, *16*(1), 371. https://doi.org/10.1186/s12864-015-1540-2

SUPPORTING INFORMATION

Additional supporting information may be found online in the Supporting Information section.

How to cite this article: Rippe JP, Dixon G, Fuller ZL, Liao Y, Matz M. Environmental specialization and cryptic genetic divergence in two massive coral species from the Florida Keys Reef Tract. *Mol Ecol*. 2021;00:1–17. https://doi.org/10.1111/mec.15931